Turkish J. Eng. Env. Sci.
31 (2007) , 79 – 87.

An in Vitro Investigation of Steady Transitional Flow in an Arteriovenous Graft-to-Vein Anastomosis

Nurullah ARSLAN
Fatih University, Graduate Institute of Sciences and Engineering and Department of Industrial Engineering, 34500, İstanbul-TURKEY
e-mail: narslan@fatih.edu.tr

Received 14.09.2006

Abstract

Fluid flow analysis was experimentally performed inside a venous anastomosis of an arteriovenous (AV) graft-to-vein connection. Velocity measurements were conducted inside an upscaled end-to-side graft model under steady flow conditions at Reynolds numbers of 1000, 1800, and 2500, which are the representatives of in vivo flow conditions at diastolic, average, and systolic phases inside a human AV graft used for dialysis access. The distribution of the velocity and turbulence intensity was measured at several locations in the plane of the bifurcation and in the plane that is perpendicular to the plane of bifurcation. Critical flow regions, such as the separation region and high turbulence region, were found inside the anastomosis.

Key words: Hemodialysis, Arteriovenous graft, Stenosis, Turbulence.

Introduction

Hemodialysis patients are in serious danger if not sustained by a kidney transplant or some form of dialysis therapy. Arteriovenous grafts (AV) made of polytetrafluoroethylene (PTFE) are used as an access site for the dialysis process. PTFE connection is performed from artery to vein. More than half of these constructions fail and require surgical reconstruction within 3 years (Kanterman et al., 1995). Most of the grafts are occluded by intimal hyperplasia (IH), which is the narrowing of the vein downstream of the graft, or stenosis. The use of AV grafts is increasing worldwide, which has led researchers to study the formation of IH and its prevention inside AV grafts. Kanterman et al. (1995) showed that hyperplastic stenosis occurs predominantly in the proximal venous segment (PVS), downstream of the graft-to-vein junction, as shown in Figure 1. This suggests the possible involvement of disturbances to flow created in the graft-to-vein junction and advected downstream. Shu et al. (1991) obtained the mean velocity profile and wall shear stress (WSS) inside realistic AV graft models. They implicated the low and oscillating WSS near the stagnation point and separation region in the development of a lesion distal to the toe (Figure 2a and b). No turbulence measurement results were presented.

Fillinger et al. (1989, 1991) measured perivascular tissue vibration and intimal thickening in AV graft venous anastomoses, investigating in separate studies the results of varying both flow-rate and geometric details. They found the highest tissue vibration and intimal thickening to be localized on the toe side of the PVS. In the absence of direct measurements of flow turbulence, they hypothesized that tissue vibration was caused by turbulent flow, and that the degree of vibration was correlated with the blood turbulence level. They concluded that a high flow rate, in a geometry tending to cause flow disturbances, led to flow instability, deposition of vibration energy in the vessel wall, venous intimal-medial thickening, and the initiation of hyperplasia.

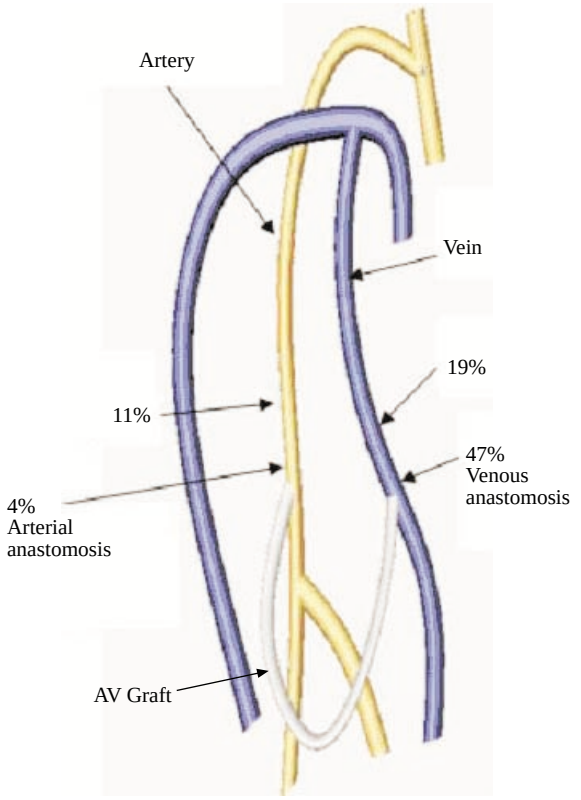

Figure 1. Distribution of hyperplastic stenoses according to Kanterman et al. (1995).

While these studies have contributed to our understanding of IH formation in anastomoses, they did not fully take into account all of the special fluid mechanical circumstances pertaining to this junction. The major differences between these 2 end-to-side anastomoses, the arterial and the venous, from the fluid mechanical point of view, relate to the higher flow-rate and the reduced viscosity for the renal dialysis access graft. Higher flow-rate is a consequence of the fact that the arteriovenous shunt bypasses the peripheral resistance, forcing the heart to increase cardiac output by virtue of the increased venous return. Higher flow rates produce a much higher Reynolds number in the graft-to-vein junction and cause a greater tendency for flow instability and turbulence, as noted by Fillinger et al. (1990). This fact is illustrated by ultrasonic measurements of flow-rates and vessel diameters in a patient with such an arteriovenous graft constructed (Figure 3). In this study, it was assumed that turbulent flow is likely in any graft-to-vein junction having the diameter and flow-rate necessary for continuing patency and dialysis use.

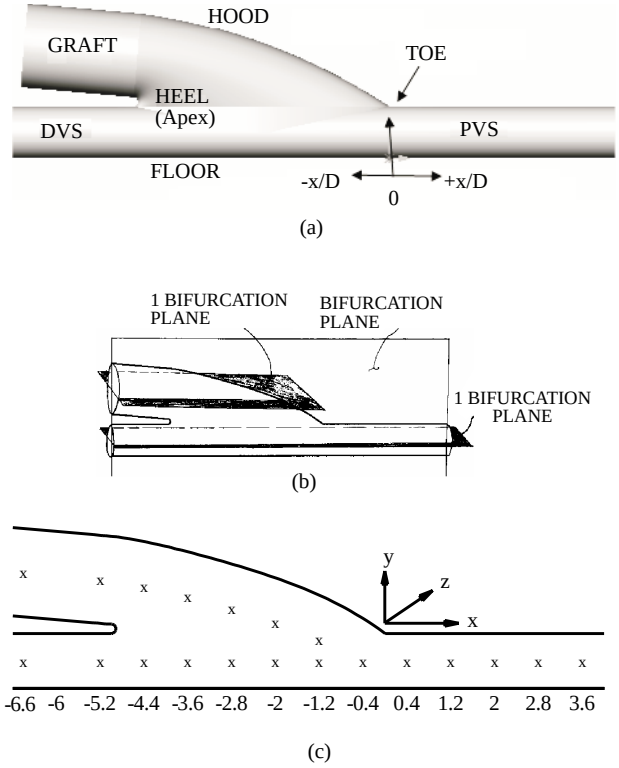

Figure 2a-c. Geometry, nomenclature (a), measurement planes (b), and measurements points (c) of the venous anastomosis AV graft model.

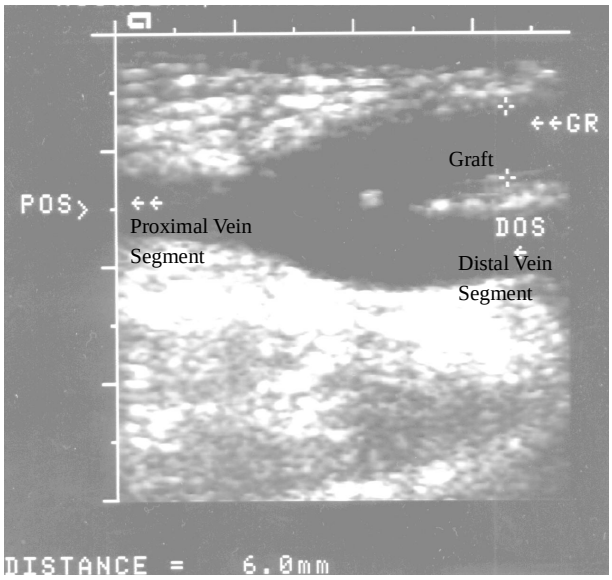

Figure 3. Ultrasonic B-mode scan of a dialysis patient's graft-to-vein junction (venous anastomosis) (Arslan, 1999).

In vivo vessel walls are exposed to 2 main hemodynamic forces or biomechanical stresses: shear stress (dragging frictional force created by blood flow and mechanical stretch) or tension, a cyclic strain stress created by blood pressure (Sou et al., 1998; Davies et al., 1999; Frangos et al., 1999). Because biomechanical stress uniquely exerts its effects on the vessel wall, it could play an important role in the development of arteriosclerosis (Hu and Xu, 2002).

The present research aimed to investigate the possible relationship between turbulence level and AV graft failure. Herein, the measurements under steady transitional flow conditions of the magnitude and spatial distribution of turbulence inside an in vitro graft model representative of the graft-to-vein junction of a dialysis AV graft are reported.

Materials and Methods

In vivo velocity measurements were obtained using color Doppler ultrasound on a dialysis patient to determine AV graft-vein junction flow condition and vessel diameter. The measurements were conducted within 1 month of graft construction. Figure 3 shows the B-scan-mode outline of the venous anastomosis in the patient. The PTFE AV graft connected the brachial artery to the basilic vein near the patient's elbow. As seen in Figure 3, the measured graft lumen diameter (D) for this patient was 6.0 mm and the angle between the graft and the vein was around 25°.

For the patient shown in Figure 4, the instantaneous mean of the sonography trace was estimated to be 1.5 m/s at the maximum and 1.0 m/s at the minimum of the cycle. For the other patient, the corresponding numbers were 1.2 and 0.8 m/s. Measurements were also obtained in the PVS and DVS; however, determination of the mean velocity was difficult because of the degree of spectral broadening.

Based on the velocity measured in the sample volume (V), and assuming normal blood viscosity (μ = 3.5 mPa s), the above measurements lead to a systolic peak Reynolds number of 2500 and a diastolic minimum of 1000 for the patient shown in Figure 3 ($Re = \rho VD/\mu$, where ρ = blood density, 1.05 g/ml).

The AV graft-to-vein connection model used in this study was that previously used by Loth et al. (1997) to investigate the hemodynamics in a distal end-to-side arterial bypass anastomosis. This model geometry also closely approximates the graft-vein junction of the AV graft. The model was scaled up 8 times relative to the in vivo case. The model material was a transparent elastomer (Sylgard 184, Dow Corning) and the walls were thick enough that the model could be considered essentially rigid. The graft-to-vein diameter ratio was 1.6, with a graft lumen diameter of 50.8 mm and a host vein diameter of 31.75 mm. The graft axis intersected the host vein axis at an angle of 5°.

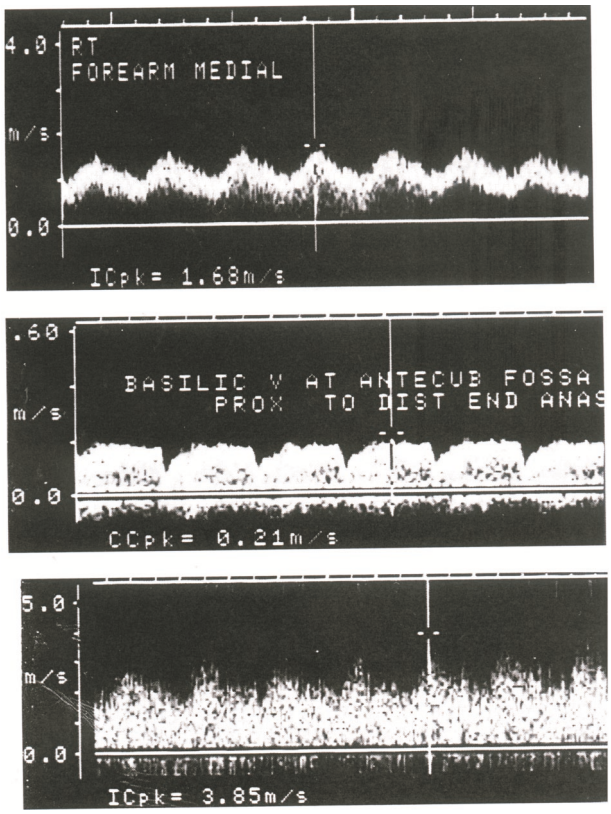

Figure 4. In vivo velocity measurements by color Doppler ultrasound at the graft inlet.

Measurements

An experimental setup was designed and constructed to provide the upscaled model with the appropriate inlet and outlet flow conditions. The fluid employed, a mixture of 42% water and 58% glycerin by weight, was chosen to match the index of refraction of the Sylgard model (n= 1.41). This fluid had a refractive index of 1.41, a density of 1.16 g/ml, and a dynamic viscosity of 10 mPa · s, as measured by a Wells-Brookfield LVTDV-II spindle type micro-viscometer at 23 °C. A $^1/_3$ hp centrifugal Teel split-phase pump provided the pressure head to drive the flow. The total flow rate was measured by bucket and stopwatch.

Clinical experience is that the vein distal to the graft-vein junction often occludes; when it remains patent, the flow rate is typically small (< 10% of the total flow rate into the venous anastomosis). The ratio of the graft inlet flow rate to the DVS inlet flow rate we used was 90:10. The DVS inlet flow rate was measured by an ultrasound transit-time flowmeter (Transonic model T101). Since fluid viscosity is sensitive to temperature, a heater/mixer in the downstream tank was used to keep the fluid temperature at 23 ± 0.5 °C during the experiments. The flow system is shown in Figure 5. The model was placed in a flow circuit under steady flow conditions such that flow entered the graft from a straight tube 4 m long with an inner diameter of 50.8 mm. Three different steady flow rates, which are the characteristics of the in vivo flow case, were set up, all with the same inlet flow ratio between the graft and the DVS. Reynolds numbers based on the graft flow-rate and graft diameter were 1000, 1800, and 2500, respectively.

Velocity profiles were measured as millimeter-spaced points along 2 perpendicular diameters of the cross section; one in the bifurcation plane and one normal to it (Figure 2c). At Re = 1000, 13 axial locations along the vein axis were examined, starting distally (upstream) at $x = -6.8D$ relative to the toe position, and extending proximally to $x = +3.6D$. Preliminary measurements revealed that the turbulent fluctuation amplitudes within the anastomotic region were comparable to or lower than those measured at the graft inlet ($x = -6.8D$). On this basis, detailed measurements for the higher Reynolds numbers were confined to the graft inlet, the furthest proximal axial location within the anastomosis, and the PVS. The 2 components of velocity were measured simultaneously with a 2-color laser system (DANTEC, mirror type F147/B073 model 5500A), which used a 350 mW argon-ion laser (blue = 488 nm, green = 514.5 nm). The 2 measured velocity components were in the plane of the bifurcation; the u-component was parallel to the vein axis and the v-component was perpendicular to it. All measurements were scaled to in vivo values ($V_{vivo} = 2.5V_{vitro}$). The ellipsoid probe volumes had diameters of 0.192 and 0.203 mm, with axial lengths of 1.66 and 1.75 mm for the blue and green beams, respectively. The particles used to scatter the laser light were 0.993-μm diameter polymer micro spheres (Duke Scientific Corporation, Palo Alto, CA, USA, cat. no. 4009B). At each measurement location, data were collected for 1-5 s in order to collect 100 points. The data were then interpolated in time to remove velocity biasing and were averaged to determine the steady flow velocity at that measurement location.

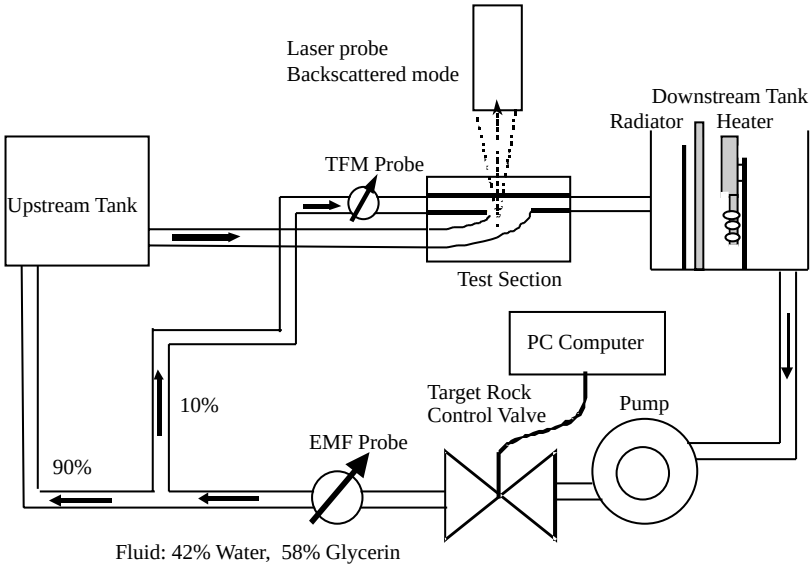

Figure 5. Experimental setup of the flow system (Arslan, 1999).

The SIZEware data acquisition program (Dantec, Inc.) was used to record the instantaneous velocity for steady flow. We recorded 5000 validated samples inside the flow field and then the mean velocity was found by taking the average of the samples for u and v components of the velocity. Since the data rate was lower near the wall of the model, an elapsed time mode was used and data were taken for 5 min (the number of the validated samples was changed from 200 to 1000). The fluctuation velocities were found by subtracting the mean velocity from the instantaneous velocities at each time step and then averaged over the specified number of validated samples to find the variables at each measurement location (Arslan, 1999).

Results

In the plane of the bifurcation Figure 6 shows velocity vectors, turbulence fluctuation amplitudes, and Reynolds stresses for Re = 1000. SI units were used, except for the Reynolds stresses, where dynes/cm^2 follows the convention established in the hemolysis and arterial wall disease literature. At $x = -6.8D$, flow enters the model via the graft and DVS with a fully developed laminar (parabolic) velocity profile. The 2 streams enter the anastomosis region and merge, accelerating as they move proximally due to the reduction in cross-sectional area. A small separation region downstream of the toe is evidenced by a retrograde vector near the wall at $x = +0.4D$. Turbulent fluctuations and Reynolds stresses are small, except near the toe side of the PVS, starting at $x = +2.0D$. The largest fluctuation amplitude (u_{rms} at $x = +2.0D$) reaches 23% of the local mean velocity. The maximum Reynolds stress value is 278 dynes/cm^2 at position $x = +2.0D$.

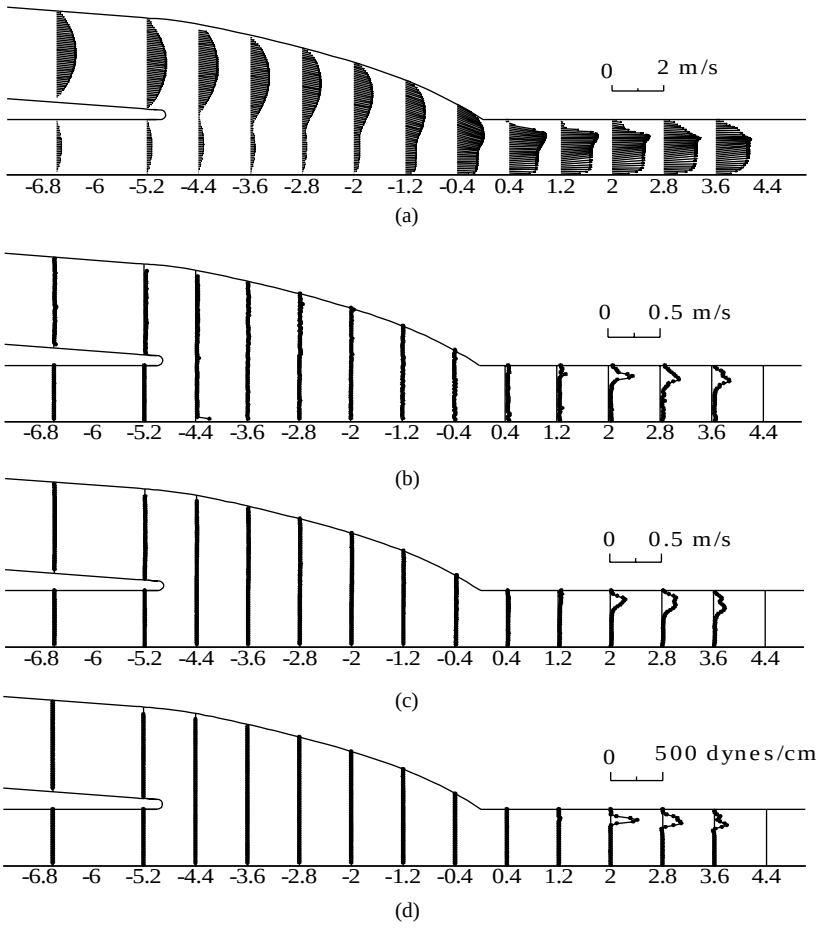

Figure 6a-d. Vector plots (a), u_{rms}(b), v_{rms}(c), and $\rho\overline{u'v'}$ (d) at Re = 1000 in the bifurcation lane.

The normally quoted threshold Re for transition in a pipe is at best approximate, and is valid only for an extremely long and smooth straight pipe. Turbulence can be tripped at lower Reynolds numbers, but cannot be sustained below about 2300. The recirculating-flow rig used here was not designed with special precautions against flow instability, since no such ideal circumstances can be assumed in biological flows. At Re = 1800 (Figure 7), a small but distinct degree of blunting of the graft inlet profile was observed, indicating the flow to be near transition. The velocity profile at the downstream (proximal) end of the anastomosis was not greatly different from that at Re = 1000, but the turbulent fluctuation amplitude was considerably higher, reflecting the fluctuation amplitude at the graft inlet. The maximum amplitude at $x = -0.4D$ reached the value of 9 cm/s (5% of the local mean velocity-compute x-sectional area and was correctly weighted average at the section) of the local mean velocity averaged over the cross-section. The separated eddy just downstream of the toe now penetrated further into the lumen at $x = -0.4D$, but reattachment occurred before $x = +1.2D$. Further downstream, the profiles generally resembled those found at Re = 1000, except that at $x = +3.6D$ the u-component profile had become blunt and almost symmetrical. Turbulent fluctuations and Reynolds stresses were elevated relative to those at Re = 1000, and reached significant amplitudes closer to the toe, at $x = +1.2D$. The maximum Reynolds stress was 902 dynes/cm^2, whereas the maximum at Re = 1000 was 278 dynes/cm^2.

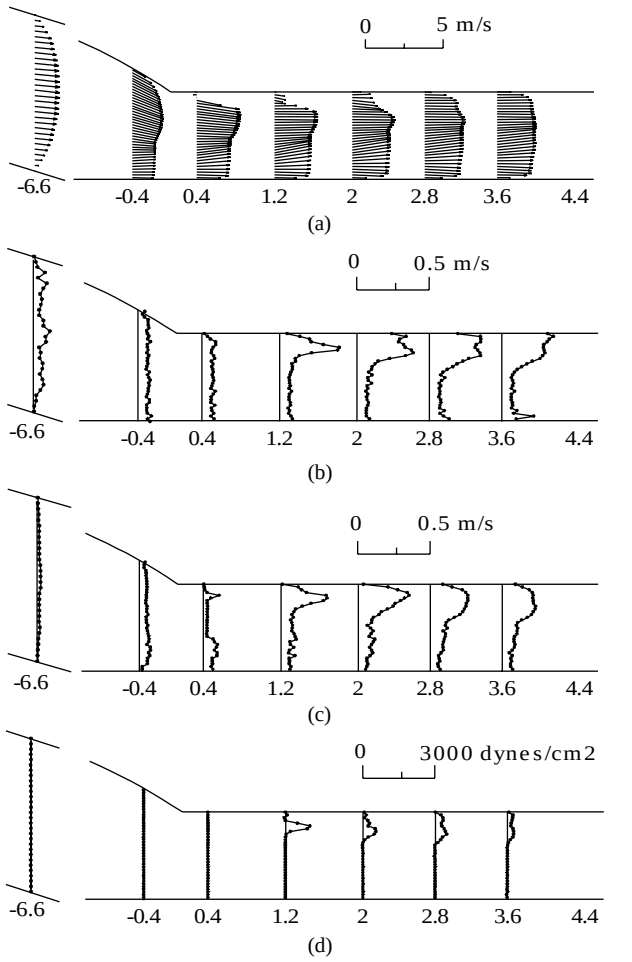

Figure 7a-d. Vector plots, (a), u_{rms}(b), v_{rms}(c), and $\rho\overline{u'v'}$ (d) at Re = 1800 in the bifurcation plane (zoomed in PVS).

At Re = 2500 (Figure 8), graft inlet flow is turbulent, with a characteristically blunt mean-velocity profile and m-shaped u_{rms} profile. Flow at the inlet of the DVS remained laminar. At the proximal end of the anastomosis region, the peak of the mean-velocity profile is shifted towards the floor. Further substantial increases in turbulence amplitudes and Reynolds stresses occur, and a second peak in fluctuation amplitude arises towards the floor side of the PVS, for both u_{rms} and v_{rms}. For u_{rms}, this second spatial peak of amplitude exceeds the primary peak at locations downstream of $x = +2.0D$. The primary u_{rms} peak is detected still closer to the toe than at Re = 1800, at $x = +0.4D$. At all 3 Reynolds numbers, the primary u_{rms} peak on the toe side itself splits into 2 as the maximum amplitude decays proximally in the PVS.

In the perpendicular plane to the bifurcation plane

The model was constructed to be symmetric about the plane of the bifurcation such that velocity profiles are expected to be symmetric about the centerline. Symmetry is evident in the profiles of velocity, turbulent fluctuation amplitudes, and Reynolds stress, as shown in Figure 9. Velocity measurements taken along lines perpendicular to the plane of the bifurcation provide detailed information on the magnitude of the secondary motion inside the anastomosis. Figure 9 shows the profiles measured for the u velocity components at various locations in the graft and vein sides at a Reynolds number of 1000. The velocity profiles in these figures are nearly symmetric about the $x-y$ plane (z= 0), as expected, due to the symmetry of the model about the midplane. The u component profiles outside the midplane on the graft side are shown in Figure 9a. At the graft entrance (po-

sition –6.8), the profile is parabolic. Once inside the anastomosis, the velocity gradient near the side walls decreases slightly at positions –5.2 to –2.8 and increases due to the decrease in the cross-sectional area of the anastomosis at positions –2 and –1.2. The u velocity component at the inlet of vein side starts as a parabolic profile, which is the characteristic profile for laminar flow, and gets blunter inside PVS (Figure 9b). The graft side v component of velocity, shown for each cross section in Figure 10a, is significantly lower in magnitude than the u component of velocity on the graft side. The v component profile is relatively flat at position –4.4, whereas the u component profile at this position is more parabolic. This indicates that flow near the sidewalls has been redirected more toward the graft floor than the near the midplane. This secondary motion is an expected result, since the fluid with lower inertia near the sidewalls is influenced more by DVS pressure gradient than higher inertia fluid near the midplane.

The $\boldsymbol{v}$ component profiles on the vein side are shown in Figure 9b. The magnitude of the $\boldsymbol{v}$ component is significantly less than that of the u component inside the DVS and PVS, and also inside the anastomosis on the vein side. At positions –4.4 and –3.6, all the flow moves proximally (positive x direction) due to the flow from the vein side. At all measurement locations, until position +1.2, the v component is directed to the floor side of the vein. At position +1.2 the v component is directed away from the floor near the midplane and towards to the floor near the sidewalls with maxima directed away from the floor located at $z = \pm$ *0.25 D*. The m-shaped profile starting at position –1.2 to +3.6 demonstrates the 3-dimensional nature of the flow field and the strong secondary motion that exist inside the anastomosis and PVS.

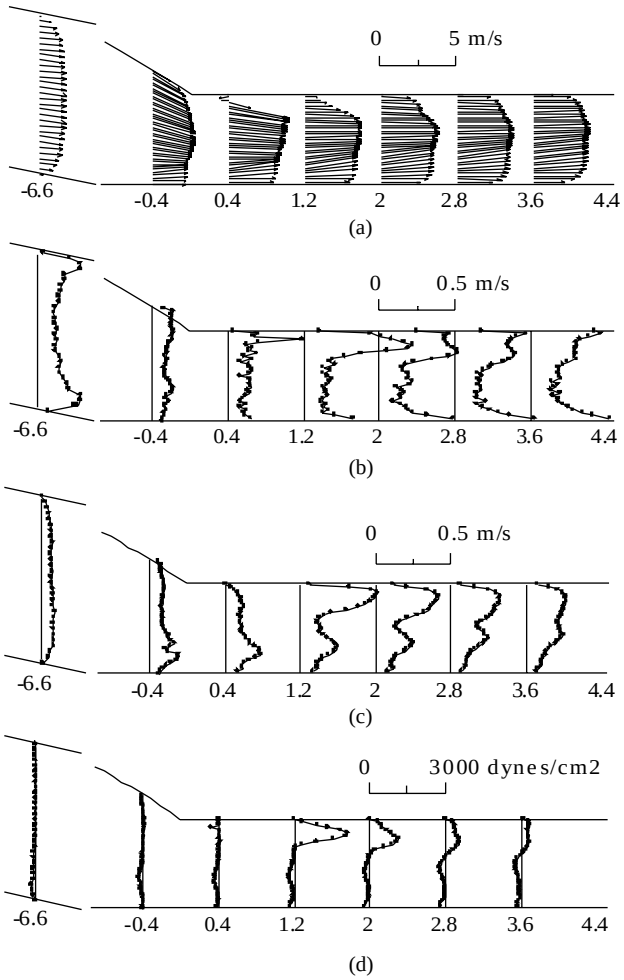

Figure 8a-d. Vector plots, (a), u_{rms}(b), v_{rms}(c), and $\overline{\rho u'v'}$ (d) at Re = 2500 in the bifurcation plane (zoomed in PVS).

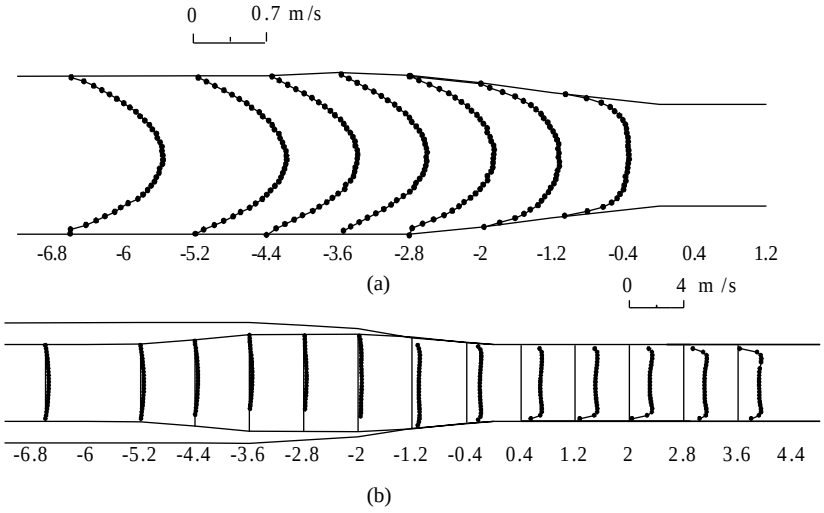

Figure 9a,b. LDA velocity measurements scaled to in vivo values outside the midplane. (a) u velocity component profiles on the graft side (0.8 D_v from the hood-midplane intersection) and (b) u velocity component profiles on the vein side (0.5 D_v from the floor-midplane intersection), Re = 1000.

Discussion and Conclusions

The results presented herein detail the nature of the flow field to be expected within the venous anastomosis of a dialysis patient's blood-access AV graft. The flow field is complex and 3-dimensional in nature, with transition to turbulence as a prominent feature. In normal arterial flows, pulsatility plays an important role, and a quasi-steady flow assumption may not apply. AV graft flows are abnormal in this respect, in that the elevated mean flow rate gives rise to a reduced pulsatility index. The results under steady flow conditions are therefore useful for several reasons. First, a low pulsatility index implies that the unsteadiness is of reduced importance. Second, steady flow provides insight into the causes of specific flow features, which may also exist in pulsatile flow, and allows them to be specifically identified as geometric phenomena rather than unsteady phenomena. Third, numerical solutions of the Navier-Stokes equations require experimental measurements for code validation. Such measurements are particularly needed for transitional flows, where numerical techniques are still unproven. The present results provide data for code validation of the 3-D steady flow solution inside a mathematically defined, but clinically realistic vascular graft geometry. This is a necessary step on the way to a pulsatile solution.

The secondary flow patterns found in the proximal vein segment (the outflow) are at first sight surprising, in that the predominant flows toward the floor are close to the lateral walls. To aid terminology, it helps to consider the graft as though the plane of the bifurcation is vertical and the floor is horizontal and at the bottom, while emphasizing that any such convention is purely arbitrary. Based on this convention, since the downward-directed stream from the graft must turn to align with the horizontal vein axis, the opposite pattern of secondary flow would be expected; the stream curvature would then suggest that the predominant downward stream in the PVS be on the anastomosis plane of symmetry, with compensating upward flows on the lateral walls. In fact, the whole secondary flow pattern is dictated by that setup when the inlet flow from the graft impinges on the anastomosis hood and is deflected downward. This stream curvature causes lateral downward flows, which persist when the same stream meets that which has arrived from the DVS. This latter stream is laminar at all flow-rates investigated, and therefore predominantly has momentum near the vein axis. This profile further aids the secondary flow pattern noted already, of upward flow in the bifurcation plane in the PVS, because the stream from the graft is able to deflect the lateral fluid more readily than that on the vein axis. A third contributing factor to this overall picture is the relatively flat profile of the inlet graft flow at all but the lowest Reynolds number; this flow has much lateral momentum already, which is deflected by the hood to form strong downward-directed lateral streams. On the other hand, a flat profile with boundary layers forms

a weaker Dean vortex flow than does a parabolic one, all other things being equal, and so flatness at the inlet from the graft has both contributory and opposing effects. Once the 2 streams merge in the PVS, the flow is undeveloped and consequently has a reduced contributing factor to the observed pattern of upward flow in the bifurcation plane. The PVS secondary flow pattern is qualitatively similar at all 3 Reynolds numbers examined, but is strongest at the intermediate Re = 1800. Reduced secondary flow tends to form the classical Dean secondary flow pattern; this counts as yet a fourth.

The distribution of turbulence inside a venous anastomosis was simulated using an upscaled in vitro model under steady flow conditions. The highest turbulent intensities and Reynolds stresses were found at the toe side of the PVS. This coincides with previously reported locations of stenosis formation in AV grafts, which implicates turbulence as a potential cause of AV graft failure. Future studies using pulsatile flow and realistic AV graft models will be conducted to further characterize the importance of turbulence. An understanding of the relationship between graft failure and turbulence levels may lead to graft design criteria to maximize AV graft patency rates.

Acknowledgments

The author acknowledges the Mechanical Engineering Department of the University of Illinois at Chicago for the use of their Laser Doppler anemometer system for experimental measurements and valuable discussions with their staff regarding the flow phenomena.

References

Arslan, N., "Experimental Characterization of Transitional Unsteady Flow inside a Graft-to-Vein Junction", Ph.D. thesis, The University of Illinois at Chicago, 1999.

Davies, P.F., Polacek, D.C., Handen, J.S., Helmke, B.P. and DePaola, N., "A Spatial Approach to Transcriptional Profiling: Mechanotransduction and the Focal Origin of Atherosclerosis", Trends Biotechnol., 17, 347-51, 1999.

Fillinger, M.F., Kerns, D.B. and Schwartz, R.A., "Hemodynamics and Intimal Hyperplasia", Chapter 2 of Vascular Access for Hemodialysis-II, W.L. Gore & Associates, Inc., and Precept Press, Inc., (B.G. Sommer and M.L. Henry, Eds.), 21-51, 1991.

Fillinger, M.F., Reinitz, E.R., Schwartz, R.A.., Resetarits, D.E., Paskanik, A.M. and Bredenberg, C.E., "Beneficial Effects of Banding on Venous Intimal-Medial Hyperplasia in Arteriovenous Loop Grafts," The American Journal of Surgery, 158, 87-94, 1989.

Fillinger, M.F., Reinitz, E.R., Schwartz, R.A., Resetarits, D.E., Paskanik, A.M., Bruch D. and Bredenberg, C.E., "Graft Geometry and Venous Intimal-Medial Hyperplasia in Arteriovenous Loop Grafts", Journal of Vascular Surgery, 11, 556-566, 1991.

Frangos, S.G., Gahtan, V. and Sumpio B., "Localization of Atherosclerosis: Role of Hemodynamics", Arch. Surg., 134, 1142-9, 1990.

Hu, Y. and Xu, Q., "New Mouse Model of Vein Bypass Graft Atherosclerosis", Heart, Lung and Circulation, 11, 182-88, 2002.

Kanterman, R.Y., Vesley, T.M., Pilgram, T.K., Guy, B.W., Windus, D.W. and Picus, D., "Dialysis Access Grafts: Anotomic Location of Venous Stenosis and Results of Angioplasty", Radiology, 195, 135-139, 1995.

Loth, F., Jones, S.A., Giddens, D.P., Bassiouny, H.S., Glagov, S. and Zarins, C.K., "Measurements of Velocity and Wall Shear stress inside a PTFE Vascular Graft Model under Steady Flow Conditions" Journal of Biomechanical Engineering, 119, 187-194, 1997.

Shu, M.C. and Hwang, N.H.C., "Haemodynamics of Angioaccess Venous Anastomoses", Journal of Biomedical Engineering, 13, 103-112, 1991.

Zou, Y., Hu, Y., Metzler, B. and Xu Q., "Signal Transduction in Arteriosclerosis: Mechanical Stress Activated MAP Kinases in Vascular Smooth Muscle Cells", Int. J. Mol. Med., 1, 827-34, 1998.